

# Electrochemical Study of 3-(*N*-alkylamino)thiophenes: Experimental and Theoretical Insights into a Unique Mechanism of Oxidative Polymerization

Christopher L. Heth,<sup>†</sup> Dennis E. Tallman,<sup>‡</sup> and Seth C. Rasmussen<sup>\*,†</sup>

Department of Chemistry and Molecular Biology, North Dakota State University, NDSU Dept. 2735, P.O. Box 6050, Fargo, North Dakota 58108-6050, and Department of Coatings and Polymeric Materials, North Dakota State University, NDSU Department 2760, P.O. Box 6050, Fargo, North Dakota 58108-6050

Received: December 31, 2009; Revised Manuscript Received: March 10, 2010

A number of conjugated polymer systems can be generated via electropolymerization, including polythiophenes and polyanilines. While both have been reported to polymerize anodically via radical coupling, the presence of the aniline nitrogen plays a significant role in the mechanism of electropolymerization. In this study, the electropolymerization mechanism of 3-(*N*-alkylamino)thiophenes, structural hybrids of thiophene and aniline, is studied utilizing experimental and theoretical methods. Synthesis of new short chain 3-(*N*-alkylamino)-thiophenes is discussed, and a mechanism of electropolymerization is proposed whereby oxidation occurs through removal of a nitrogen lone pair electron, followed by a chemical step resulting in radical contribution at the 2-position of the thiophene ring. Coupling of these final radical cations thus results in a typical poly( $\alpha$ - $\alpha'$ -thiophene) backbone.

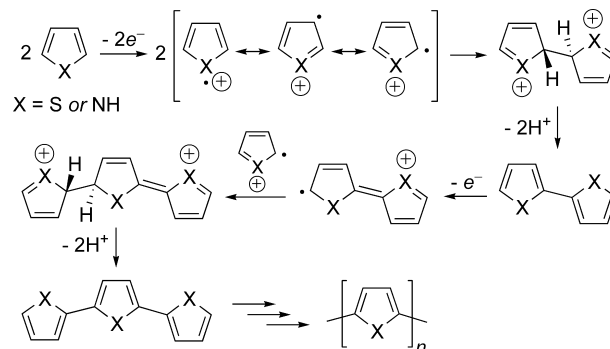
## Introduction

Conjugated organic materials continue to generate intense interest due to their desirable physical and electronic properties combined with the ability to tune those properties at the molecular level through synthetic modification.<sup>1</sup> Of these materials, a number of systems can be generated via electrochemical polymerization, including the commonly studied polythiophenes, polypyrroles, and polyanilines.<sup>2–12</sup> While the electrochemical synthesis of these materials has been examined, the bulk of these studies have focused on the effects of side chains on the resultant polymer, with only a handful of now dated studies exploring the mechanism of polymerization.<sup>2–10</sup>

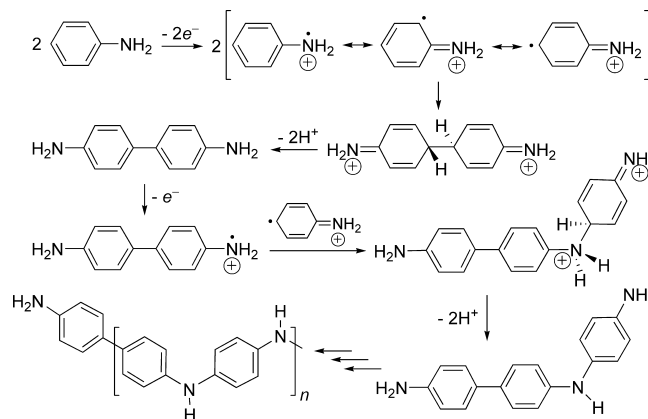
It is commonly held that thiophenes and pyrroles polymerize anodically through the removal of an electron from the heterocyclic  $\pi$ -system to form the corresponding radical cation (Scheme 1).<sup>2–6</sup> While multiple resonance forms are possible, spin density studies support the localization of the unpaired electron at the  $\alpha$ -position.<sup>4,6</sup> Coupling of the radical cations thus occurs predominately through the  $\alpha$ -positions, followed by deprotonation to give the neutral dimer.<sup>2–6</sup> Chain propagation then continues through sequential oxidation, coupling, and deprotonation steps.

The polymerization of aniline is similar but with some important differences.<sup>7–10</sup> Here, oxidation of the aniline nitrogen results in the formation of the corresponding radical cation, which again can exist in multiple resonance forms (Scheme 2). Unlike the heterocycles above, however, spin density studies of the aniline radical cation indicate nearly equal distribution of the unpaired electron between the nitrogen and the *para* carbon of the benzene ring.<sup>10</sup> As such, this provides the opportunity for three possible couplings: nitrogen–nitrogen (head-to-head, HH); nitrogen–arene (head-to-tail, HT); arene–arene (tail-to-tail, TT).<sup>7,8</sup> If HH coupling occurs, the resulting

## SCHEME 1: Oxidative Polymerization Mechanism of Thiophene and Pyrrole



## SCHEME 2: Oxidative Polymerization Mechanism of Aniline

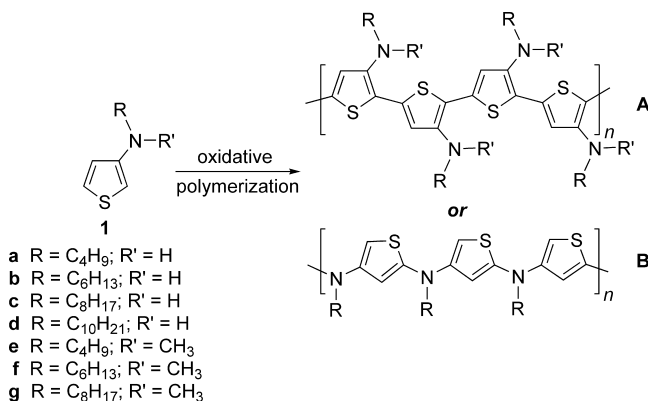


diarylhydrazine intermediate is not stable and quickly undergoes conversion to other species via either disproportionation or the benzidine rearrangement,<sup>13</sup> particularly under acidic conditions. As such, HH coupling does not contribute to polymer formation.<sup>7</sup> Of the two remaining possibilities, TT coupling is

\* To whom correspondence should be addressed. E-mail: seth.rasmussen@ndsu.edu.

<sup>†</sup> Department of Chemistry and Molecular Biology.

<sup>‡</sup> Department of Coatings and Polymeric Materials.

**CHART 1: Oxidative Polymerization of 3-(*N*-Alkylamino)thiophenes**


predominant at high concentrations of the initial radical cation.<sup>8</sup> As this is the case for most polymerization conditions, the initial couple is most likely to be TT, followed by deprotonation to give the neutral dimer. As with the heterocycles above, chain propagation then continues through sequential oxidation, coupling, and deprotonation steps. As the initial TT dimer formed can only couple through the nitrogens,<sup>9</sup> the additional chain propagation steps would favor HT coupling.

Over the last several years, our group has been studying the synthesis and polymerization of 3-(*N*-alkylamino)thiophenes (**1**, Chart 1),<sup>14–18</sup> which can be viewed as structural hybrids of traditional 3-functionalized thiophenes and *N*-alkylanilines. As such, one of the original questions was whether these thiophenes would oxidatively polymerize to produce a conventional poly( $\alpha$ - $\alpha'$ -thiophene) (Chart 1, structure **A**) or if polymerization would result in a polyaniline-type structure (structure **B**). While NMR characterization of polymerization products is not consistent with structure **B** and supports the production of a conventional polythiophene backbone,<sup>16</sup> recent work in our lab suggests that this may not be occurring via the standard mechanism illustrated in Scheme 1 above.<sup>18</sup>

As seen in Figure 1, the analysis of 3-(*N*-octylamino)-thiophene (**1c**) by cyclic voltammetry (CV) reveals two distinct anodic peaks, the first at +440 mV (vs Ag/Ag<sup>+</sup>) with another near the edge of the solvent window at +2600 mV.<sup>18,19</sup> Additionally, while both oxidations are electrochemically irreversible, two broad cathodic peaks can be observed, both of which are coupled to the initial oxidation process. This suggests

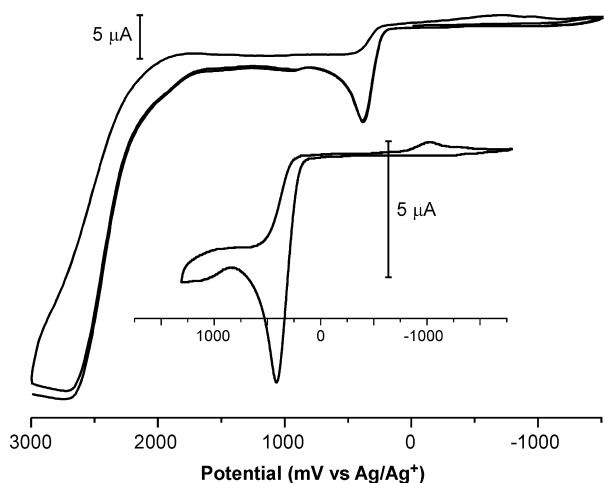


**Figure 1.** Cyclic voltammogram of **1c**; 100 mV/s scan rate.

**TABLE 1: Functional Group Effects on First Peak Potential of Oxidation**

|  | R   | E <sub>ox</sub> <sup>a</sup> (V) | Reference |
|--|---|----------------------------------|-----------|
|  | H   | 1.95                             | 20        |
|  | CH <sub>2</sub> OC <sub>6</sub> H <sub>13</sub> | 1.83                             | 12        |
|  | C <sub>8</sub> H <sub>17</sub>                  | 1.50                             | 21        |
|  | CH <sub>3</sub>                                 | 1.52                             | 13        |
|  | OC <sub>6</sub> H <sub>13</sub>                 | 1.29                             | 12        |
|  | NHC <sub>8</sub> H <sub>17</sub> ( <b>1c</b> )  | 0.43                             | 18        |

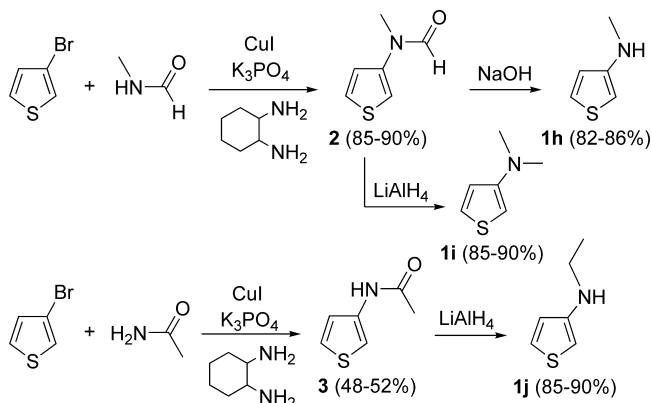
<sup>a</sup> Potentials vs Ag/Ag<sup>+</sup>; values adjusted to account for differing reference electrodes.

that a chemical process follows the initial oxidation that results in a new redox-active species. When compared to a variety of 3-substituted thiophenes (Table 1), it is apparent that 3-(*N*-alkylamino)thiophenes have lower potentials of oxidation than can be explained solely by the electron-donating character of the amine functionality. Such observations led us to propose that the initial oxidation consisted of the removal of a nitrogen lone pair electron in analogy to aniline as discussed above.<sup>18</sup> This occurrence could account for both the decreased potential of oxidation and the observation of two oxidation processes. However, we have also shown that this first oxidation can lead to polymerization under constant potential conditions, which raises questions about both the true nature of this oxidation and the overall polymerization mechanism involved in the generation of the resulting poly(*N*-alkylaminothiophene)s.<sup>18</sup> Herein, we utilize experimental and theoretical studies to further investigate the redox processes of 3-(*N*-alkylamino)thiophenes and deduce a unique mechanism for their oxidative polymerization.

**Results and Discussion**

**Synthetic Strategy.** To help provide further insight into the possibility of a unique mechanism for oxidative polymerization, molecular modeling was utilized for comparison to experimental results. Due to the computational complications associated with modeling the geometries of long alkyl chains, it was desirable to synthesize short chain analogues of 3-(*N*-alkylamino)-thiophenes in order to provide the best comparisons between experimental and computational results. However, the production of such species required a new synthetic strategy, as the gaseous short chain amine reagents are not compatible with the reflux conditions of previously utilized amination methods.<sup>14,18,22</sup> The desired compounds could however be easily produced through copper-catalyzed amidation of thiophene,<sup>23</sup> followed by reduction<sup>24</sup> or hydrolysis to produce 3-(*N*-methylamino)-thiophene (**1h**), 3-(*N,N*-dimethylamino)thiophene (**1i**), and 3-(*N*-ethylamino)thiophene (**1j**) in good yields (Scheme 3).

**Electrochemistry.** The electrochemical data for the new aminothiophenes **1h–j** are given in Table 2 along with various longer chain analogues for comparison. As with the CV of **1c** above, the analysis of **1h** shows two electrochemically irreversible oxidations with *E*<sub>pa</sub> values of +0.44 and ~ +2.5 V (vs Ag/Ag<sup>+</sup>). Examination of CVs of **1j** at increasing scan rates (Figure 2) reveals significant shifts in potential for the first oxidation (from +0.41 V at 100 mV/s to +0.60 V at 900 mV/s), further illustrating electrochemical irreversibility. In addition, two broad reduction waves are coupled to the first oxidation, centered around −0.45 and −0.96 V, also in good agreement with the CV of **1c** seen in Figure 1. The presence of these reduction waves coupled to the electrochemically irreversible oxidation suggests the presence of some chemical process undertaken by the oxidized product to produce species which can be electrochemically reduced. Sequential CV cycles exhibit no new redox

**SCHEME 3: Synthesis of Short Chain 3-(*N*-Alkylamino)thiophenes**

couples, and NMR analyses of analyte samples following sequential CV cycles reveal no detectable oligomer formation and little to no degradation of the initial monomer. The combination of these results suggests that the initial oxidations and subsequent reduction processes in 3-(*N*-alkylamino)-thiophene systems follow a square scheme, as illustrated in Scheme 4.

Still unclear, however, is the lack of cathodic current relative to the anodic current seen under CV conditions. The reduction is clearly coupled to the initial oxidation, and therefore, the most likely causes for this reduced cathodic response are diffusion of oxidized product away from the electrode surface or coupling reactions consuming oxidation products prior to reduction. Further study will be necessary to determine the exact causes of this behavior.

While the potentials of the second oxidation for all studied 3-(*N*-alkylamino)thiophenes are considerably more positive than the  $\sim +2.0$  V reported for unfunctionalized thiophene,<sup>20</sup> this is consistent with the presence of charge following the first oxidation, making removal of an additional electron more difficult. As shown in Table 2, the extension of the alkyl chain length has little to no effect on either oxidation.

In order to investigate the origin of the first observed oxidation, **1i** was studied to determine the effect of substitution of the amine hydrogen with an electron-donating methyl group. The substitution resulted in an 80 mV shift to lower potential which is in good agreement with potentials previously reported for **1g**.<sup>18</sup> The effect of the methyl substitution is consistent with a nitrogen-based oxidation, as this substitution would have only a minor electronic effect on the thiophene ring and its thiophene-based oxidation.

In an attempt to confirm the origin of the first oxidation as nitrogen-based, **1g** was then quaternized through methylation to produce *N,N*-dimethyl-*N*-octyl-*N*-(3-thienyl)ammonium iodide (**4**) as previously reported.<sup>18</sup> As binding of the lone pair electrons should prohibit nitrogen oxidation at observable potentials, **4** should not exhibit the low potential oxidation observed for the previous aminothiophenes if the nitrogen-based assignment proposed above is correct. As shown in Figure 3, the CV of **4** exhibits a single oxidation ( $E_{pa} = +1.8$  V) consistent with a traditional thiophene oxidation. However, it was not clear if the low potential oxidation was eliminated or simply shifted to higher potential due to the presence of the charged quaternary nitrogen. The minor reversible redox waves seen at low potential were attributed to the iodide counterion. This was further confirmed by comparison to the CV of KI, as shown in Figure 3.

To remove any last doubts as to the origin of this initial oxidation, **1i** was analyzed by CV in the presence of a small amount of  $\text{BF}_3$ -etherate. The addition of  $\text{BF}_3$  should bind the nitrogen lone pair through formation of the  $\text{BF}_3$  adduct, without the generation of any net positive charge. Thus, any change in the initial oxidation could be attributed to direct interaction with the nitrogen lone pair, rather than electrostatic forces resulting from any charge on the aminothiophene. As seen with **4** above, the low potential oxidation was not observed (Figure 4), with the first oxidation occurring near +1.8 V. Additionally, the reductions coupled to the low potential oxidation were also absent, with the only observed reduction originating from the  $\text{BF}_3$ -etherate in solution. The formation of the nitrogen- $\text{BF}_3$  adduct was confirmed by  $^1\text{H}$  NMR (Figure 5), which shows deshielding of protons in the 2- and 4-positions of the thiophene ring relative to pure **1i**. Additional comparison to **4** indicates a lack of formal charge on the nitrogen in the  $\text{BF}_3$  adduct, as evidenced by the significant downfield positions of the aromatic peaks for the charged thiophene **4**. The combination of the NMR and CV results supports the assignment of the low potential oxidation of 3-(*N*-alkylamino)thiophenes to be the removal of a lone pair electron from the nitrogen center.

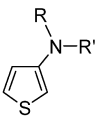
**Hammett Plots.** In order to help understand the observed electrochemical behavior of 3-(*N*-alkylamino)thiophenes in relation to other substituted thiophenes, Hammett relationships were investigated for the oxidation of various thiophenes. Hammett  $\sigma_p^+$  values have been used previously in the literature to correlate the electronic effects of functional groups to the anodic peak potential of the thiophene monomer.<sup>2,12</sup> In 1986, Waltman and Bargon reported a linear correlation for a series of 3-functionalized thiophenes limited to electron-withdrawing groups. The linear fit of that study was taken to indicate a uniform electronic process characterized as monomer oxidation through removal of an electron from the  $\pi$ -system of the thiophene ring.<sup>2</sup> Using a combination of published  $\sigma_p^+$  values for a variety of functional groups<sup>25</sup> and the corresponding first oxidation  $E_{pa}$  of the respective thiophenes, the previous data set has now been expanded to contain both electron-withdrawing and electron-donating substituents, including the aminothiophenes of interest here. As shown in Figure 6, this combined data set gives a slope of 0.83 that matches quite well with the previous  $\rho_\pi$  value of 0.80 determined by Waltman and Bargon<sup>2</sup> and retains the previously observed linear correlation between  $E_{pa}$  and  $\sigma_p^+$ .

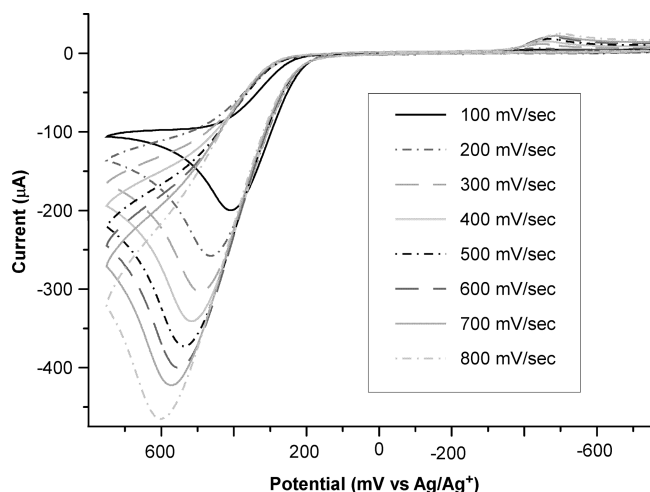
The electronic effect described by the Hammett  $\sigma_p$  values include both field/inductive (*F*) and resonance (*R*) components, as described by the relationship<sup>25</sup>

$$\sigma_p = F + R$$

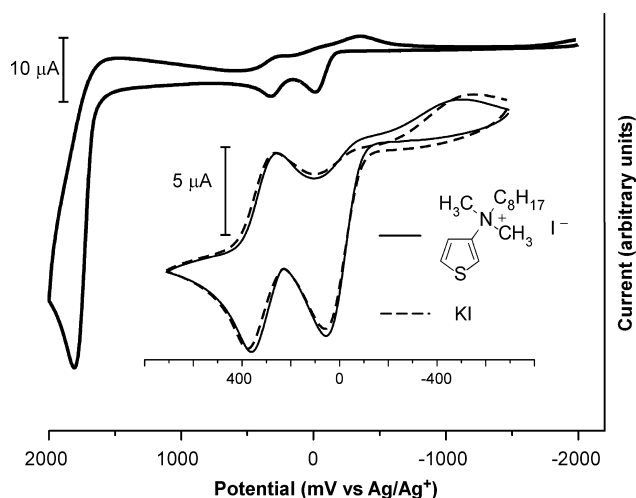
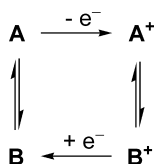
As inductive effects represent the primary contribution to changes in the potential of thiophene oxidation, a greater understanding of functional group effects can be obtained by plotting literature values of *F* vs  $E_{pa}$  for the same set of substituents. As shown in Figure 7, this reveals a strong linear correlation, with the exception of electron-donating groups containing either lone pairs or a  $\pi$ -electron system.<sup>25</sup> While a greater resonance contribution would be expected for these outliers, a reasonable correlation can also be observed within this isolated subset (including halo-, methylmercapto-, thienyl-, alkoxy-, and amido-thiophenes), suggesting these species all share a similar resonance contribution to  $\sigma_p$ . Of particular interest, however, is that 3-(*N*-methylamino)- and 3-(*N,N*-dimethylamino)thiophenes do not correlate well with either of

TABLE 2: Electrochemical Data for 3-(*N*-Alkylamino) and 3-(*N,N*-Dialkylamino)thiophenes<sup>a</sup>

|  | Compound  | R                              | R'              | E <sub>ox</sub> <sup>1</sup> (V) | E <sub>ox</sub> <sup>2</sup> (V) |
|---|-----------|--------------------------------|-----------------|----------------------------------|----------------------------------|
|   | <b>1h</b> | CH <sub>3</sub>                | H               | 0.44                             | 2.5                              |
|   | <b>1i</b> | CH <sub>3</sub>                | CH <sub>3</sub> | 0.36                             | 2.2                              |
|   | <b>1j</b> | C <sub>2</sub> H <sub>5</sub>  | H               | 0.44                             | 2.5                              |
|   | <b>1a</b> | C <sub>4</sub> H <sub>9</sub>  | H               | 0.43                             | 2.5                              |
|   | <b>1c</b> | C <sub>8</sub> H <sub>17</sub> | H               | 0.43                             | 2.6                              |
|   | <b>1g</b> | C <sub>8</sub> H <sub>17</sub> | CH <sub>3</sub> | 0.33                             | 2.1                              |

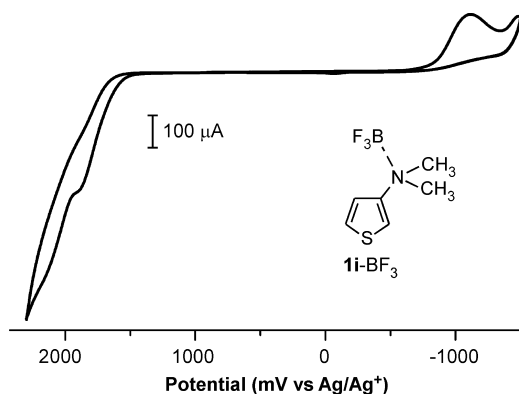
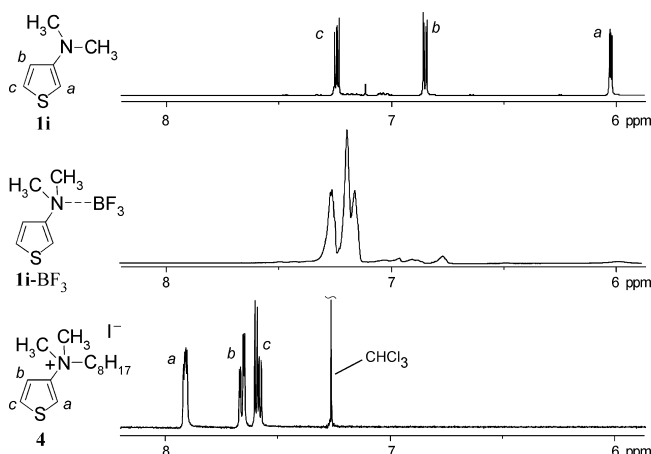
<sup>a</sup> Potentials vs Ag/Ag<sup>+</sup>.Figure 2. CV of **1j** at various scan rates.

## SCHEME 4: General Square Mechanistic Scheme

Figure 3. Cyclic voltammogram of **4** with comparison to KI (inset); 100 mV/s scan rate.

the two groups described above, potentially indicating an even greater resonance contribution for these aminothiophene species.

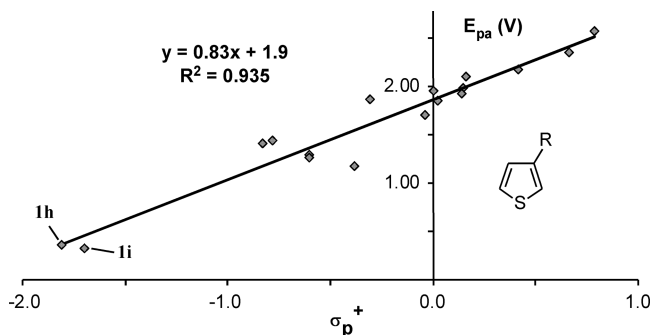
**Molecular Modeling.** Before theoretical models could be utilized to study 3-(*N*-alkylamino)thiophenes, the optimized geometry of unfunctionalized aniline was determined using a number of computational methods (DFT, HF, MP2) with a

Figure 4. Cyclic voltammogram of **1i**-BF<sub>3</sub> adduct; 100 mV/s scan rate.Figure 5. Aromatic <sup>1</sup>H NMR chemical shifts.

variety of basis sets (6-31G+(d) and larger) for comparison to experimentally determined structural parameters.<sup>27</sup> While most methods showed good agreement with the experimentally determined bond lengths and angles, DFT calculations utilizing a B3LYP correlation functional with a 6-311G+(dp) basis set showed a slightly better overall fit while also requiring significantly lower computational costs compared to larger basis sets and *ab initio* methods. Comparison to other DFT methods previously utilized for modeling substituted thiophene systems also shows a slight improvement in bond length prediction utilizing B3LYP/6-311G+(dp) methods.<sup>10</sup> With this in mind, all further molecular modeling was performed using these methods.

Examination of the optimized geometry of **1h** reveals a pyramidal geometry about the nitrogen atom in the neutral state (Figure 8). In the monocationic state, however, a change from pyramidal to planar geometry is observed, resulting in a completely coplanar molecule. This suggests that, in the neutral state, the nitrogen lone pair orbital has predominately sp<sup>3</sup> character and minimal overlap with the thiophene π-system,





**Figure 6.** Hammett plot of the oxidation of 3-functionalized thiophenes.<sup>26</sup>

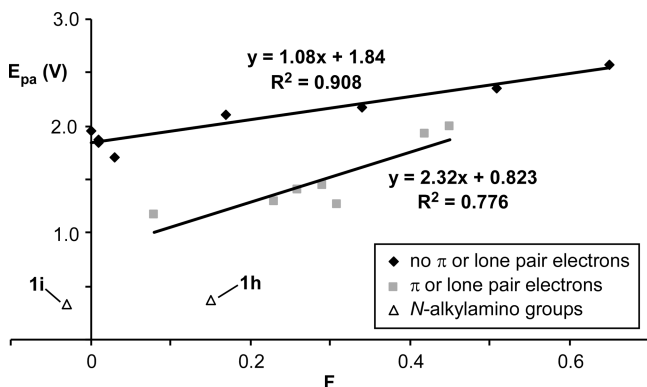


**Figure 7.** Plot of *F* vs  $E_{pa}$  for 3-functionalized thiophenes with various side chains.<sup>26</sup>

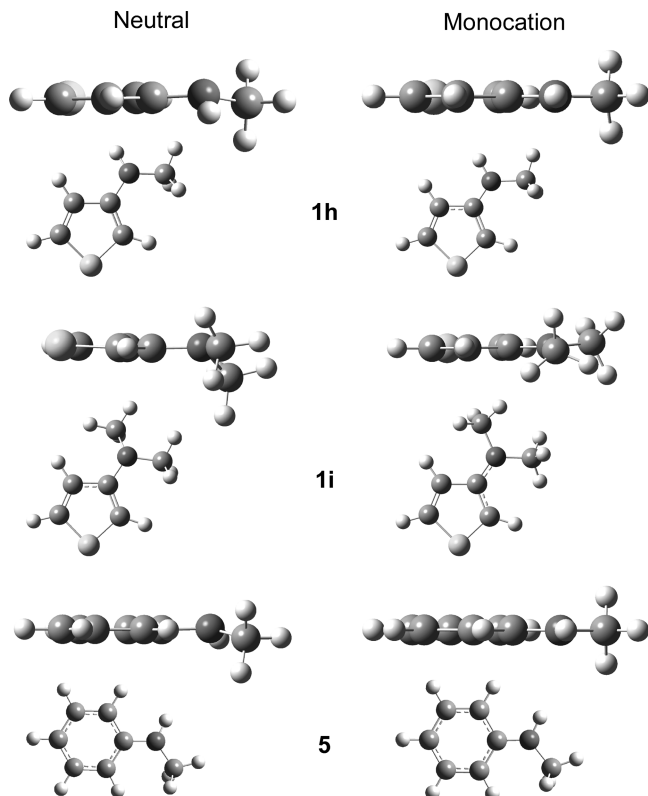


**Figure 8.** Optimized geometries of neutral and cationic **1h**, **1i**, and **5**.

while in the cationic state the nonbonding orbital is almost entirely p in character and in good conjugation with the ring. This geometry change is even more pronounced in the case of **1i** due to the larger dihedral angle about the nitrogen center in

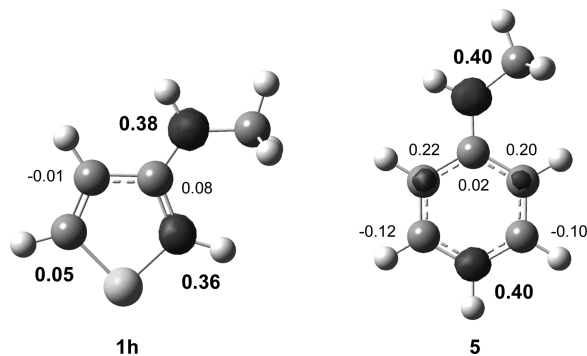


**Figure 9.** Mulliken spin density calculations for **1h** and **5**.

the neutral state, and compares well with the geometry changes observed for *N*-methylaniline (**5**) and *N,N*-dimethylaniline using the same modeling methods.

Applying these models to the observed CV behavior, the electrochemical irreversibility of the anodic peak may be due to this geometry change. Electrochemical oxidation of the neutral species, followed by conversion to the more planar geometry, may result in a new electrochemically reducible species. Comparison of calculated energies of the cationic state in each of these geometries ( $A^+ \rightarrow B^+$ , Scheme 4) reveals an energetic difference of 35.4 kJ/mol, favoring the planar geometry and providing a significant thermodynamic driving force for its generation. Electrochemical reduction of this new species, followed by conversion back to the pyramidal geometry, reforms the original species. The predicted energetic difference for the conversion between the two neutral species ( $B \rightarrow A$ , Scheme 4) was calculated to be 19.2 kJ/mol. As regeneration of the neutral thiophene after oxidation would require not only reduction but also both energetically favored geometric conversions ( $A^+ \rightarrow B^+ \rightarrow B \rightarrow A$ , Scheme 4), the reduction process would be expected to require less energy than the corresponding oxidation, equal to the sum of the energies of the two proposed chemical steps (54.6 kJ/mol). Examination of the onset potentials for oxidation and reduction from the CV in Figure 2 shows a difference of ~550 mV (~53 kJ/mol), in good agreement with the calculated energies. Through this series of electrochemical and chemical steps, the system would be overall chemically reversible under CV conditions, providing an explanation for the lack of polymer formation observed in previous studies.<sup>18</sup>

Mulliken spin density calculations were then performed for monocationic aniline, **5** and **1h** (Figure 9). Aniline showed good agreement with the previous literature study,<sup>10</sup> with similar results seen for the methyl analogue **5**. Here, equal contribution to Mulliken spin density was predicted for the nitrogen (0.40) and the *para*-carbon of the ring. In comparison, nearly equal spin density contributions in **1h** are seen on the amine nitrogen (0.38) and the carbon in the 2-position of the thiophene ring (0.36). It should also be noted the calculated contribution to spin density on the 5-position of the thiophene ring (0.05) is considerably reduced relative to the 2-position. This likely contributes to the high degree of regioregularity observed in electropolymerized 3-(*N*-alkylamino)thiophenes.<sup>16</sup>

**Electrochemical Modeling.** The electrochemical behavior of **1h** at a scan rate of 500 mV/s was modeled using the Digisim 3.03 software package. This scan rate was chosen to allow sufficient experimental cathodic currents for comparison to the model. The observed CV behavior could be modeled using electrochemical (E) and chemical (C) steps to simulate an ECEC mechanism (Figure 10). This supports the presence of an electrochemically irreversible oxidation, followed by a chemical

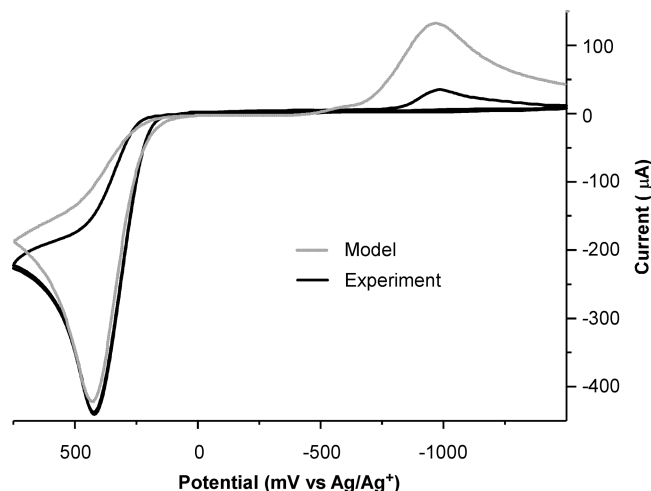


Figure 10. CV modeling of **1h**; 500 mV/s scan rate.

step to form a new reducible species, which can then undergo further electrochemical and chemical changes to reform the starting species. As demonstrated previously for **1j**, the first anodic and cathodic peak potentials are dependent upon the scan rate, suggesting slow electron transfer kinetics. This is supported through the need to include significant anodic and cathodic overpotentials (310 and 240 mV, respectively) in order to model the observed CV behavior. Small rate constants on the order of  $10^{-6}$  cm/s were used for anodic electron transfer steps in order to properly model the electrochemical response. Rate constants of  $\sim 10^{-3}$  cm/s were used for cathodic electron transfer steps.

Of particular note, however, is the discrepancy between the electrochemically modeled reduction current and the cathodic current observed under CV conditions. This suggests there may be another process occurring that is not included in these models, potentially diffusion processes, coupling reactions, or some combination thereof. Attempts to include such processes in the electrochemical models did not improve the fit of the models to experimental data.

**Proposed Mechanism.** On the basis of the studies above, an overall mechanism for the oxidative polymerization of 3-(*N*-alkyl amino)thiophenes is proposed in Scheme 5. As presented, oxidation of the monomer occurs through removal of a nitrogen lone pair electron. A chemical step in the form of a change in nitrogen geometry ( $sp^3$  to  $sp^2$ ) follows, resulting in an increased overlap of the singly occupied nitrogen orbital with the  $\pi$ -system of the thiophene ring. This new planar geometry allows better electronic communication between the nitrogen center and the ring, resulting in additional radical contribution on the 2-position of the thiophene ring via resonance, as demonstrated by the spin-density calculations above.

Analogous to the oxidative coupling of aniline,<sup>7,8</sup> the equal spin density between the nitrogen and the 2-position of the thiophene would then provide three possible couplings: nitrogen–nitrogen, nitrogen–thiophene, and thiophene–thiophene. However, during all electrochemical conditions investigated, no evidence of nitrogen-based coupling was ever detected. This is perhaps not unexpected, as any nitrogen–nitrogen coupled products would suffer the same instability issues of other diarylhydrazines and if formed would quickly undergo conversion via either disproportionation or the benzidine rearrangement.<sup>13</sup> The predicted products of the benzidine rearrangement would be equivalent to the thiophene–thiophene coupled products and thus even the detection of secondary products would be very difficult. As a result, the primary coupling of

radical cations occurs through the respective 2-positions and subsequent deprotonation results in formation of the head-to-head (HH) dimer, 3,3'-bis(*N*-alkylamino)-2,2'-bithiophene (**6**). The formation of **6** during electropolymerization has been repeatedly seen, and its detection and isolation from the oxidative degradation of alkylaminothiophenes during their preparation and purification is common (see the Supporting Information).<sup>18</sup>

The oxidation of **6** would then generate a new radical cation for continued chain growth. However, whether oxidation here is initially nitrogen based as in the monomeric species or simple oxidation of the bithiophene backbone is yet unclear. Electrochemical measurements of isolated samples of **6** show two oxidations at +260 and +510 mV. The higher potential value agrees well with the measured bithiophene oxidation of +490 mV for the analogous 3,3'-dimethoxy-2,2'-bithiophene.<sup>28</sup> However, the higher electron-donating ability of the amino groups could be enough to drop the bithiophene oxidation to the initial observed potential of +260 mV. Mulliken spin density calculations of **6** predict near equal spin density on one amine nitrogen (0.20) and the exterior  $\alpha$ -carbon of the opposite thiophene ring (0.23), which still suggest a significant contribution of the nitrogens to the electrochemistry of **6**. Nevertheless, coupling of **6** with monomeric radical cations would be expected to occur via head-to-tail (HT) thiophene–thiophene coupling to generate the corresponding trimeric intermediate. Sequential coupling steps through a chain growth mechanism would then lead to the formation of regioregular poly(3-(*N*-alkylamino)thiophene) as previously reported.<sup>16</sup>

## Conclusion

Monomeric 3-(*N*-alkylamino)thiophenes can be viewed as hybrids of traditional 3-functionalized thiophenes and *N*-alkylanilines. In comparison to other 3-functionalized thiophenes, these hybrid species exhibit significantly lower potentials of oxidation, which detailed electrochemical studies have now demonstrated to be due to an initial oxidation of the amine nitrogen, rather than oxidation of the thiophene  $\pi$ -system. In addition, theoretical modeling of these systems has predicted a change in geometry around the nitrogen center associated with oxidation similar to that predicted for aniline analogues, as well as an aniline-like equal distribution of calculated Mulliken spin densities between the amine nitrogen and the thiophene ring. However, considering the significant amount of aniline character exhibited by the 3-(*N*-alkylamino)thiophenes, oxidative polymerization still occurs via  $\alpha$ – $\alpha'$ -coupling to generate a typical polythiophene backbone. This combination of aniline and thiophene features results in a unique mechanism for the oxidative polymerization of these hybrid systems, blending aspects of the generally accepted polymerization mechanisms for 3-substituted thiophene and *N*-alkylaniline systems. This study reveals the effects of utilizing new reactive functional groups in conventional polymeric systems, which will become increasingly important as more advanced and complex conjugated polymeric materials are explored and applied to new device applications.

## Experimental Section

**Materials and Instrumentation.** Compounds **4**, **1c**, **1g**, and 2-isobutyrylcyclohexanone were prepared using previously reported procedures.<sup>18,22</sup> Tetrabutylammonium hexafluorophosphate (TBAPF<sub>6</sub>) was purified by literature procedures.<sup>29</sup> Acetonitrile for the electrochemical studies was purified by fractional distillation over CaH<sub>2</sub>. Dry Et<sub>2</sub>O was prepared via





100 mL flask and cooled in an ice bath.  $\text{LiAlH}_4$  (1.0 M in  $\text{Et}_2\text{O}$ , 6 mL, 6 mmol) was then added dropwise by syringe (**WARNING:  $\text{H}_2$  gas evolution**). The resulting mixture was allowed to warm to room temperature, stirred for 1.5 h, and then worked up and purified as above for **1i**. Yield 85–90%.  $^1\text{H}$  NMR (400 MHz):  $\delta$  7.15 (dd,  $J = 5.2, 2.8$  Hz, 1H), 6.61 (dd,  $J = 5.2, 1.6$  Hz, 1H), 5.96 (dd,  $J = 2.8, 1.6$  Hz, 1H), 3.55 (br, 1H), 3.12 (q,  $J = 7.2$  Hz, 2H), 1.26 (t,  $J = 7.2$  Hz, 3H).  $^{13}\text{C}$  NMR (400 MHz):  $\delta$  149.1, 125.3, 120.2, 95.7, 41.1, 15.2.

**Acknowledgment.** The authors thank the donors of The Petroleum Research Fund, administered by the American Chemical Society, for support of this research. Additional support was provided by AFOSR (DET, Grants F49620-02-1-0398, FA9550-06-1-0461, and FA9550-07-1-0370) and North Dakota State University. Thanks also to Dr. Chad M. Amb for helpful synthetic discussions.

**Supporting Information Available:** Complete table of  $\sigma_p^+$ ,  $F$ , and  $E_{\text{pa}}$  values used in the Hammett correlations, further synthetic details, and electrochemical modeling parameters. This material is available free of charge via the Internet at <http://pubs.acs.org>.

## References and Notes

- (1) (a) *Semiconducting Polymers: Chemistry, Physics and Engineering*; Hadzioannou, G.; van Hutten, P. F., Eds.; Wiley-VCH: Weinheim, Germany, 2000. (b) *Handbook of Oligo- and Polythiophenes*; Fichou, D., Ed.; Wiley-VCH: Weinheim, Germany, 1999. (c) *Handbook of Conducting Polymers*, 3rd ed.; Skotheim, T. A.; Reynolds, J. R., Eds.; CRC Press: Boca Raton, FL, 2007.
- (2) Waltman, R. J.; Bargon, J. *Can. J. Chem.* **1986**, *64*, 76.
- (3) Genies, E. M.; Bidan, G.; Diaz, A. F. *J. Electroanal. Chem.* **1983**, *149*, 101.
- (4) Waltman, R. J.; Bargon, J. *Tetrahedron* **1984**, *40*, 3963.
- (5) John, R.; Wallace, G. G. *J. Electroanal. Chem.* **1991**, *306*, 157.
- (6) Smith, J. R.; Cox, P. A.; Campbell, S. A.; Ratcliffe, N. M. *J. Chem. Soc., Faraday Trans.* **1995**, *91*, 2331.
- (7) (a) Wei, D.; Kyarnstrom, C.; Lindfors, T.; Kronberg, L.; Sjöholm, R.; Ivaska, A. *Synth. Met.* **2006**, *156*, 541. (b) Yonezawa, S.; Kanamura, K.; Takehara, Z. *J. Electrochem. Soc.* **1993**, *140*, 629. (c) Seo, T. E.; Nelson, R. F.; Fritsch, J. M.; Marcoux, L. S.; Leedy, D. W.; Adams, R. N. *J. Am. Chem. Soc.* **1966**, *88*, 3498.
- (8) Hand, R. L.; Nelson, R. F. *J. Am. Chem. Soc.* **1974**, *96*, 850.
- (9) D'Eramo, A. H.; Silber, J. J.; Sereno, L. *J. Electroanal. Chem.* **1995**, *382*, 85.
- (10) D'Aprano, G.; Proynov, E.; Leboeuf, M.; Leclerc, M.; Salahub, D. R. *J. Am. Chem. Soc.* **1996**, *118*, 9736.
- (11) Bryce, M. R.; Chissel, A. D.; Smith, N. R. M.; Parker, D.; Kathirgamanathan, P. *Synth. Met.* **1988**, *26*, 153.
- (12) Waltman, R. J.; Diaz, A. F.; Bargon, J. *J. Electrochem. Soc.* **1984**, *131*, 1452.
- (13) (a) Buncel, E. *Can. J. Chem.* **2000**, *78*, 1251. (b) Buncel, E.; Cheon, K.-S. *J. Chem. Soc., Perkin Trans. 2* **1998**, 1241. (c) Shine, H. J.; Park, K. H.; Brownawell, M. L.; San Filippo, J. *J. Am. Chem. Soc.* **1984**, *106*, 7077. (d) Shine, H. J.; Haddas, J.; Kwart, H.; Brechbiel, M.; Horgan, A. G.; San Filippo, J. *J. Am. Chem. Soc.* **1983**, *105*, 2823. (e) Shine, H. J. *J. Phys. Org. Chem.* **1989**, *2*, 491.
- (14) Ogawa, K.; Radke, K. R.; Rothstein, S. D.; Rasmussen, S. C. *J. Org. Chem.* **2001**, *66*, 9067.
- (15) Stafford, J. A.; Rothstein, S. D.; Tallman, D. E.; Rasmussen, S. C. *Polym. Prepr.* **2004**, *45*, 181.
- (16) Ogawa, K.; Stafford, J. A.; Rothstein, S. D.; Tallman, D. E.; Rasmussen, S. C. *Synth. Met.* **2005**, *152*, 137.
- (17) Rothstein, S. D. M.S. Thesis, North Dakota State University, Fargo, ND, 2006.
- (18) Heth, C. L.; Rothstein, S. D.; Tallman, D. E.; Rasmussen, S. C. *Polym. Prepr.* **2007**, *48*, 95.
- (19) The significantly increased current response of the second oxidation is due to overlapping contributions from the solvent oxidation at these high potentials.
- (20) Rasmussen, S. C.; Pickens, J. C.; Hutchison, J. E. *Chem. Mater.* **1998**, *10*, 1990.
- (21) Roncali, J.; Garreau, R.; Yassar, A.; Marque, P.; Garnier, F.; Lemaire, M. *J. Phys. Chem.* **1987**, *91*, 6706.
- (22) Shafir, A.; Buchwald, S. L. *J. Am. Chem. Soc.* **2006**, *128*, 8742.
- (23) Klapars, A.; Huang, X.; Buchwald, S. L. *J. Am. Chem. Soc.* **2002**, *124*, 7421.
- (24) Outurquin, F.; LeRouge, P.; Paulmier, C. *Bull. Soc. Chim. Fr.* **1986**, *2*, 259.
- (25) Hansch, C.; Leo, A.; Taft, R. W. *Chem. Rev.* **1991**, *91*, 165.
- (26) A complete table of Hammett  $\sigma_p^+$ ,  $F$ , and  $E_{\text{pa}}$  values used, including references, can be found in the Supporting Information.
- (27) Naumov, V. A.; Tafipol'skii, M. A.; Naumov, A. V.; Samdal, S. *Russ. J. Gen. Chem.* **2005**, *75*, 923.
- (28) Dietrich, M.; Heinze, J. *J. Am. Chem. Soc.* **1990**, *112* (5), 1425.
- (29) Armarego, W. L. F.; Perrin, D. D. *Purification of Laboratory Chemicals*, 4th ed.; Butterworth-Heinemann: Boston, MA, 1998; p 330.
- (30) Larson, R. C.; Iwamoto, R. T.; Adams, R. N. *Anal. Chim. Acta* **1961**, *25*, 371.
- (31) Frisch, M. J.; Trucks, G. W.; Schlegel, H. B.; Scuseria, G. E.; Robb, M. A.; Cheeseman, J. R.; Montgomery, J. A., Jr.; Vreven, T.; Kudin, K. N.; Burant, J. C.; Millam, J. M.; Iyengar, S. S.; Tomasi, J.; Barone, V.; Mennucci, B.; Cossi, M.; Scalmani, G.; Rega, N.; Petersson, G. A.; Nakatsuji, H.; Hada, M.; Ehara, M.; Toyota, K.; Fukuda, R.; Hasegawa, J.; Ishida, M.; Nakajima, T.; Honda, Y.; Kitao, O.; Nakai, H.; Klene, M.; Li, X.; Knox, J. E.; Hratchian, H. P.; Cross, J. B.; Adamo, C.; Jaramillo, J.; Gomperts, R.; Stratmann, R. E.; Yazyev, O.; Austin, J. A.; Cammi, R.; Pomelli, C.; Ochterski, J. W.; Ayala, P. Y.; Morokuma, K.; Voth, G. A.; Salvador, P.; Dannenberg, J. J.; Zakrzewski, V. G.; Dapprich, S.; Daniels, A. D.; Strain, M. C.; Farkas, O.; Malick, D. K.; Rabuck, A. D.; Raghavachari, K.; Foresman, J. B.; Ortiz, J. V.; Cui, Q.; Baboul, A. G.; Clifford, S.; Cioslowski, J.; Stefanov, B. B.; Liu, G.; Liashenko, A.; Piskorz, P.; Komaromi, I.; Martin, R. L.; Fox, D. J.; Keith, T.; Al-Laham, M. A.; Peng, C. Y.; Nanayakkara, A.; Challacombe, M.; Gill, P. M. W.; Johnson, B.; Chen, W.; Wong, M. W.; Gonzalez, C.; Pople, J. A. *Gaussian 03*, revision B.05; Gaussian, Inc.: Pittsburgh, PA, 2003.
- (32) Ah-Kow, G.; Paulmier, C.; Pastour, P. *Bull. Soc. Chim. Fr.* **1976**, *1*–2, 151–160.

JP912287S